Retrievals of Atmospheric Temperature and Water Vapor Profiles in the Arctic

James C. Liljegren[1], Maria P. Cadeddu[1], and Andrew Pazmany[2]

[1]Argonne National Laboratory, 9700 South Cass Avenue, Argonne, IL 60439, USA
Tel. +1-630-252-9540, Email: jcliljegren@anl.gov

[2]ProSensing, Inc., 107 Sunderland Road, Amherst, MA 01002, USA

***Abstract*—We show that by incorporating brightness temperature measurements at off-zenith angles, the accuracy of linear statistical retrievals of temperature and water vapor density profiles can be improved. This improvement is limited to clear sky cases where measurements at all angles represent the same atmospheric conditions. We present contribution functions and error amplification factors to show how the off-zenith measurements affect the retrieval performance.**

We also show that by combining brightness temperature measurements near the 22.235-GHz water vapor line with measurements near the 183.31-GHz line into a physical retrieval, the accuracy of the retrieved water vapor density profile for very low water vapor conditions can be significantly improved.

I. Introduction

The Atmospheric Radiation Measurement (ARM) Program has operated a twelve-channel microwave radiometer profiler (MWRP) [1] since February 2004 at its North Slope of Alaska (NSA) field site near Barrow, Alaska. The MWRP has five channels in the 22- to 30-GHz range and seven channels in the 50- to 60-GHz range that are used to derive vertical profiles of water vapor density and temperature, as well as the integrated precipitable water vapor and cloud liquid water path, at 5-minute intervals. These profiles are a valuable supplement to the collocated radiosondes launched Monday-Friday, once per day, at 2300 UTC.

Contours of temperature and water vapor density obtained by using the MWRP are presented in Fig. 1, revealing details of a frontal passage. In contrast to radiosondes, the MWRP provides substantially improved temporal resolution but coarser vertical resolution that declines in proportion to the height above ground level. A consequence of declining resolution with height is that temperature inversions, as illustrated in Fig. 1, and sharp water vapor gradients can be difficult for passive profilers to resolve accurately. In this paper, we investigate improving the vertical resolution of temperature and water vapor density retrievals by adding off-zenith measurements. We also investigate the benefits of adding measurements near 183 GHz for improving the water vapor density profile retrieval.

This work was supported by the Climate Change Research Division, U.S. Department of Energy, Office of Science, Office of Biological and Environmental Research, under contract W-31-109-Eng-38, as part of the Atmospheric Radiation Measurement Program. Argonne National Laboratory is operated by The University of Chicago for the U. S. Department of Energy.

II. Multi-Angle Retrievals

In addition to zenith, brightness temperatures are measured at elevation angles of 23.6°, 19.5°, and 16.6° symmetrically about the zenith for all K-band (22.235, 23.035, 23.835, 26.235, and 30.0 GHz) and V-band (51.25, 52.28, 53.85, 54.94, 56.66, 57.29, 58.80 GHz) channels. These angles correspond to air masses (= 1/sin(elev)) of 2.5, 3.0, and 3.5. Although these angles were selected to provide data for tipping-curve calibrations of the K-band channels [2], they may also provide a means to improve the vertical resolution of the retrieved profiles [3,4] despite not being optimally selected for this purpose.

A. Retrieval Development

We developed *a priori* statistical retrievals for temperature and water vapor density profiles by using zenith measurements only and by using zenith plus off-zenith measurements as follows. Vaisala RS90 radiosondes launched during 2002-2005 were input to a microwave radiation transfer model [5] to compute brightness temperatures at the twelve measurement frequencies and four measurement angles. The model incorporates the Rosenkranz absorption model for oxygen and water vapor [6,7], modified to use a narrower half-width for the 22-GHz water vapor line [8,9] and the MT-CKD water vapor continuum formulation [10]. K-band brightness temperatures were transformed to opacity by using mean radiation temperatures for each frequency and angle fitted to surface temperature, pressure, and relative humidity. Gaussian noise (mean = 0 K, standard deviation = 0.5 K) was added to the calculated brightness temperatures to simulate an actual instrument. The *a priori* data were divided into four periods: spring (March-May), summer (June-August), fall (September-November), and winter (December-

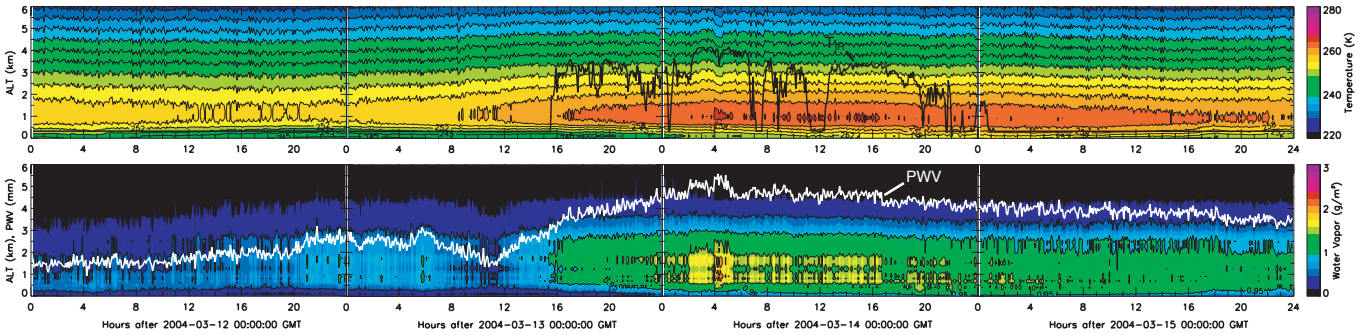

Figure 1. Time-height contours of temperature (top) and water vapor density (bottom) for 12-15 March 2004 at the ARM NSA site at Barrow, AK. The black line in the top panel indicates the temperature reported by the infrared thermometer. The white line in the bottom panel indicates the precipitable water vapor.

February). Retrieval coefficients for each season were determined by using the calculated K-band and V-band observables plus the surface pressure, temperature, and water vapor density.

To understand the effect of the off-zenith channels, the contribution functions [11] were determined by perturbing the brightness temperature at each frequency and angle in succession by 1 K, then calculating the resulting change in the retrieved temperature or water vapor density profile. To more clearly illustrate the differences between the zenith-only and multi-angle retrievals, the contribution functions for the multi-angle retrievals were summed over all angles for each frequency. The contribution functions for temperature, presented in Fig. 2, clearly show that the multi-angle retrieval contributions for the five upper V-band channels (53.85, 54.94, 56.66, 57.29, 58.80 GHz) are at lower levels. This is especially true at 53.85 GHz, which could degrade retrieval performance in the middle troposphere. The contribution of the 52.28-GHz channel to the zenith-only retrieval is negligible, whereas a small contribution is evident for the multi-angle retrieval; the 51.25-GHz channel contribution is very nearly the same for both retrievals. The contributions of the K-band channels in the upper troposphere are greater for the multi-angle retrieval. The contribution functions for water vapor density, presented in Fig. 3, show little difference between zenith-only and multi-angle retrievals for the V-band channels, which is not surprising. The contributions of the 22.235-, 23.835-, and 26.235-GHz channels are qualitatively similar for both retrievals, although greater for the multi-angle retrieval. The lower- and middle-tropospheric contributions at 23.035 and 30.0 GHz are much greater for the multi-angle retrieval.

The square root of the sum of squares of the contribution functions gives the error amplification factor [11]. The error amplification factors indicate how an error of 1 K root-mean-square (RMS) in the measured brightness temperatures would affect the RMS of the retrieved quantities. These are presented in Fig. 4. For temperature, the multi-angle retrieval may be expected to yield a reduced error below 2 km but an increased error above this level. Below 1.5 km, the RMS error in the multi-angle vapor retrieval may be greater than the zenith-only retrieval.

B. Retrieval Application

Several measurement issues must be addressed before applying the multi-angle retrievals. First, sky conditions must be horizontally uniform to ensure all angles are acquiring

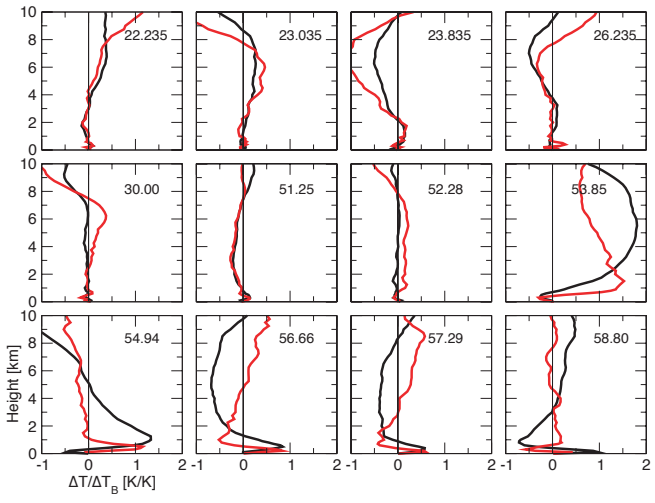

Figure 2. Contribution functions for the zenith-only (black) and multi-angle (red) temperature profile retrievals. All graphs have the same scale.

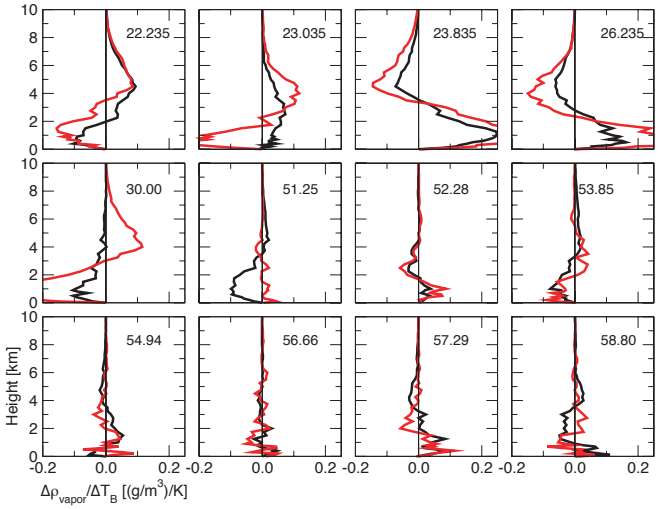

Figure 3. Contribution functions for the zenith-only (black) and multi-angle (red) water vapor density profile retrievals. All graphs have the same scale.

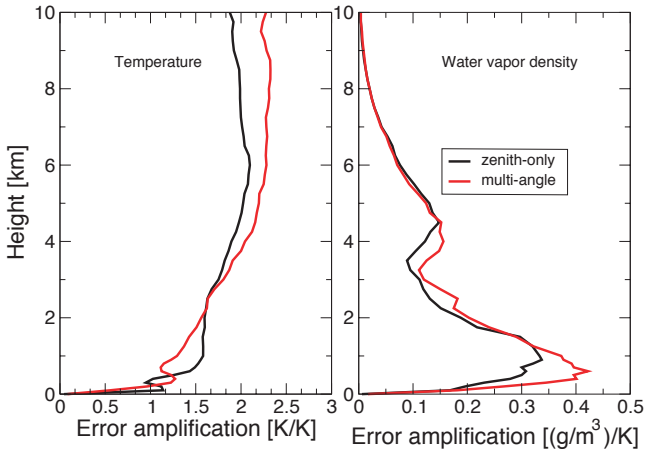

Figure 4. Error amplification factors for zenith-only (black) and multi-angle (red) retrievals of temperature (left) and water vapor density (right).

equivalent measurements. To enforce this condition, for each frequency, the square root of the sum of the squares of the brightness temperature differences between pairs of symmetric off-zenith angles had to be less than 4 K. This effectively limited measurements to clear sky conditions. Box plots of these RMS differences are presented in the upper panel of Fig. 5. The trend in these results suggested a slight tilt in the radiometer. This was confirmed by computing the RMS brightness temperature differences of model calculations at the nominal angles ± 0.5° as shown in the bottom panel in Fig. 5. The calculations show the actual tilt is considerably less than 0.5°. To account for the tilt, the brightness temperatures of the symmetrical angle pairs were averaged before applying the multi-angle retrievals.

A correction [2] was applied to the off-zenith K-band brightness temperature to account for the finite beam width of the radiometer antenna, which introduces a positive bias in the measured brightness temperatures that increases as the elevation angle decreases. The V-band measurements require no correction because the beam width at the V-band frequencies (~2°) is much less than for the K-band channels (~4.5-6°).

C. Retrieval Results

The retrievals were applied to brightness temperatures measured with the MWRP and compared with 196 radiosondes launched in close proximity to the radiometer between April 2004 and January 2006. In addition to having to screen the cases on the basis of the RMS difference of the off-zenith angle measurements described earlier, the surface temperatures measured by the radiometer and the radiosonde had to agree within 3 K, and the 10-µm infrared sky temperature had to be less than 225 K.

The ensemble mean (bias) and standard deviation of the differences (retrieval minus radiosonde) are presented in Fig. 6. Significant biases between the retrievals and radiosondes are evident. For temperature, the multi-angle retrieval exhibits a greater bias than the zenith-only retrieval,

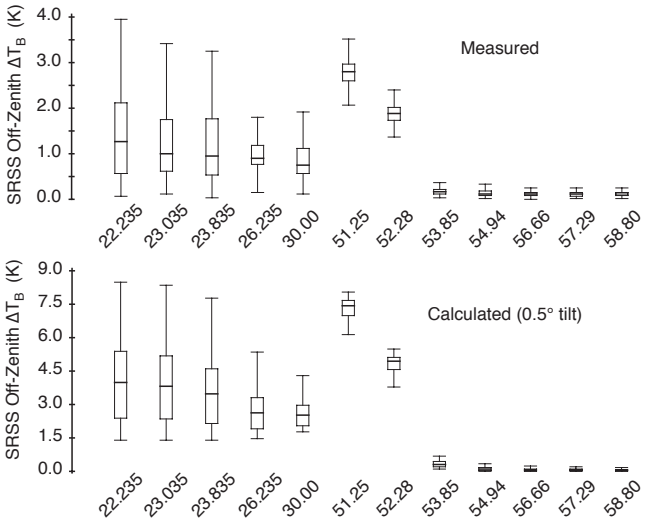

Figure 5. Box plots of the square root of the sum of the squares (SRSS) of the brightness temperature differences of the off-zenith angle pairs, $[(23.6° - 156.4°)^2 + (19.5° - 159.5°)^2 + (16.6° - 163.4°)^2]^{1/2}$ from measurements (top), and from model calculation for a 0.5° tilt (bottom).

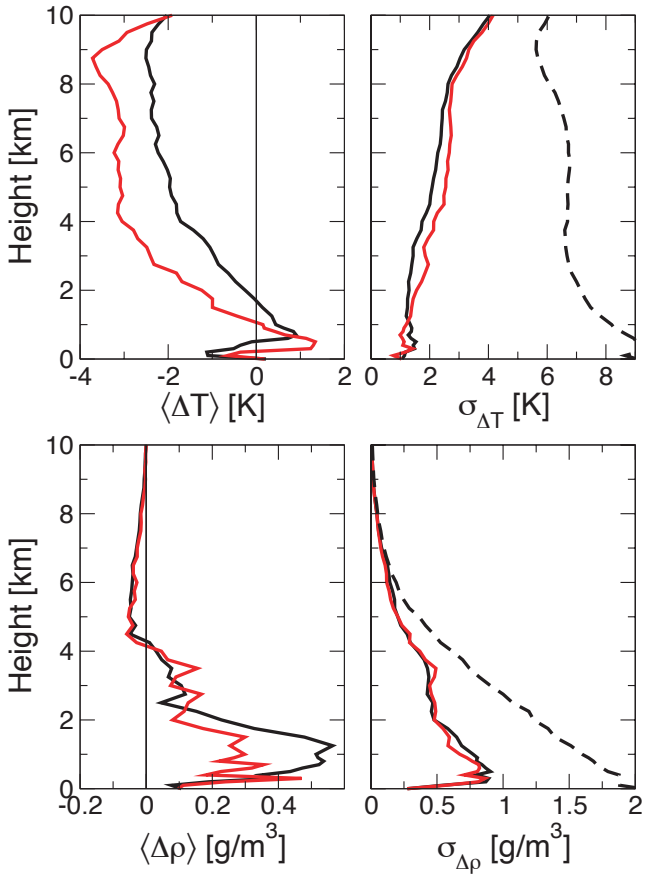

Figure 6. Mean (bias) and standard deviation of the retrieval-radiosonde differences in the temperature and water vapor profiles for the zenith-only retrievals (solid black line) and the multi-angle retrievals (red line). The standard deviation of the ensemble of radiosonde soundings around the mean of the ensemble is provided for reference (dashed black line).

whereas for water vapor density, the zenith-only retrieval has the larger bias. As the contribution functions illustrate, biases between the brightness temperatures measured by the radiometer and the model-calculated brightness temperatures used to derive the retrievals will result in biases in the retrieved temperature and water vapor density. Biases between the measured and model-calculated brightness temperatures for these frequencies and angles are presented in Table 1. The biases in the five K-band channels increase with increasing atmospheric path (i.e., with decreasing elevation angle), which suggests a calibration problem may be the cause. In contrast, the biases in the 51.25-, 52.28-, and 53.85-GHz channels decrease with increasing path length, which suggests a spectroscopic problem may be the cause [12]. Although the bias at 52.28 GHz is the largest V-band bias, its effect on the temperature retrievals is small (negligible for the zenith-only retrieval). As the contribution functions show, the bias at 53.85 GHz is the most serious. Fig. 7 shows the dramatic reduction in the temperature retrieval bias, and some improvement in the water vapor density bias, resulting from subtracting the biases at 51.25, 52.28, and 53.85 GHz. Additionally subtracting the K-band biases, as shown in Fig. 8, marginally improves the multi-angle temperature retrieval but does not improve the zenith-only temperature retrieval. The bias in the zenith-only water vapor retrieval actually increases above 2 km. This occurs because the brightness temperature errors probably arise from a calibration problem and therefore represent a scaling error rather than an offset error that can be subtracted.

TABLE I
MEASURED–MODELED BRIGHTNESS TEMPERATURE BIAS (K)

Frequency (GHz)	90°	23.6°	19.5°	16.6°
22.235	0.60	2.01	2.55	2.21
23.035	0.66	2.11	2.65	2.44
23.835	0.79	2.29	2.85	2.69
26.235	0.65	1.36	1.85	1.88
30.0	0.49	1.80	2.28	2.27
51.25	-1.61	0.59	0.67	-0.26
52.28	-3.08	-0.96	-0.84	-1.24
53.85	-1.26	-0.20	-0.04	0.01
54.94	0.22	0.39	0.45	0.46
56.66	-0.52	-0.44	-0.36	-0.33
57.29	-0.22	-0.21	-0.14	-0.12
58.80	-0.83	-0.78	-0.71	-0.71

Fig. 9 presents a comparison of zenith-only and multi-angle retrievals compared with a radiosonde for 25 April 2005. The measured biases at 51.25, 52.28, and 53.85 GHz were subtracted before applying the retrievals. In this case, the multi-angle retrievals demonstrate improved accuracy over the zenith-only retrievals.

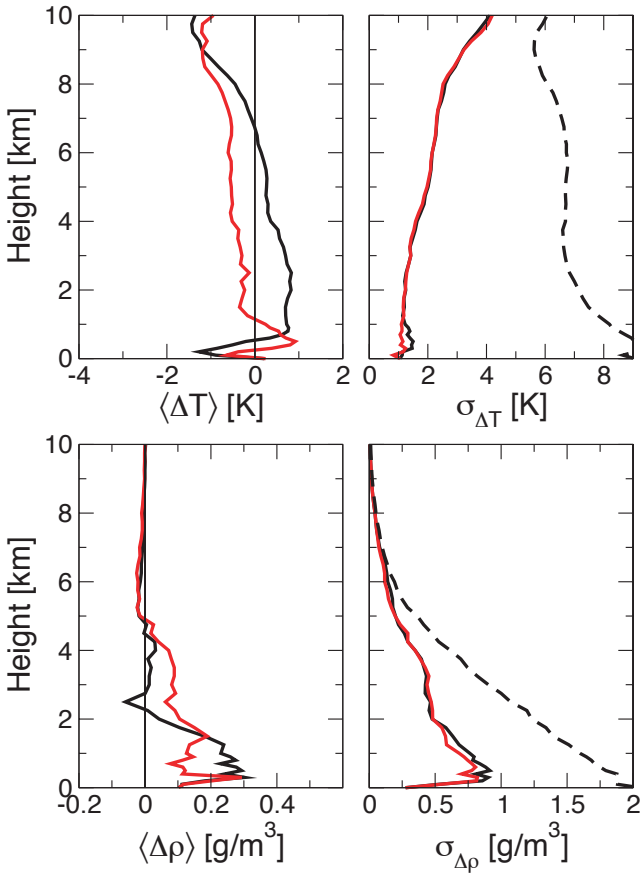

Figure 7. Same as for Fig. 6, except the biases at 51.25, 52.28, and 53.85 GHz listed in Table 1 have been subtracted before applying the retrievals.

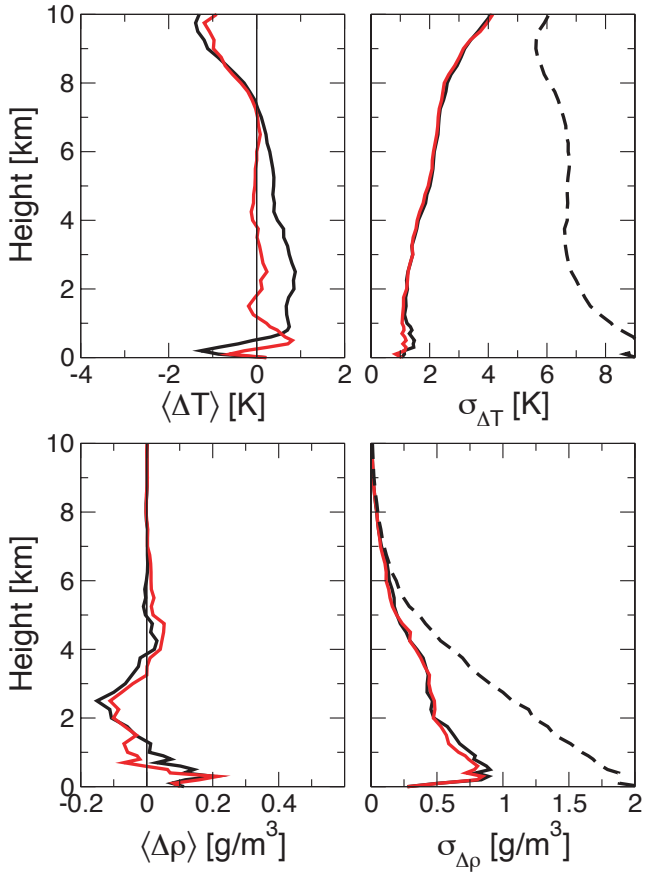

Figure 8. Same as for Fig. 7, except the biases at all five K-band channels listed in Table 1 have additionally been subtracted before applying the retrievals.

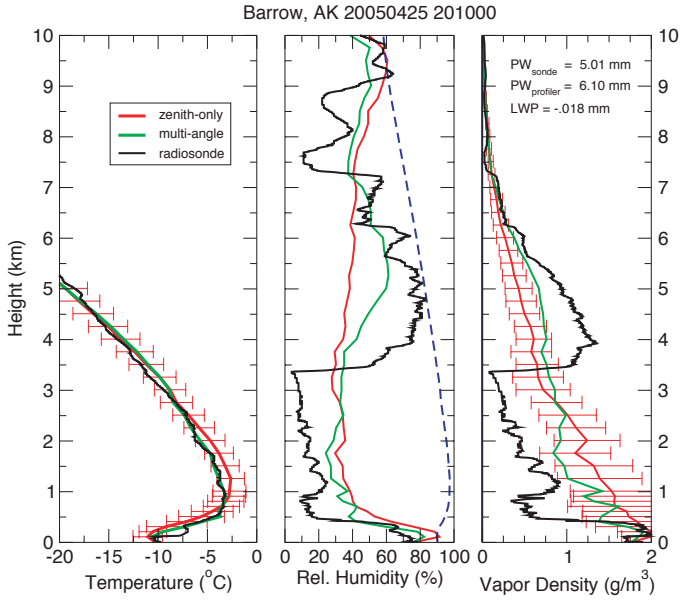

Figure 9. Profiles of temperature (left panel) and water vapor density (right panel) derived by using the zenith-only (red) and multi-angle (green) retrievals compared with radiosonde. The relative humidity (center panel) is calculated by using the retrieved temperature and water vapor density. The ratio of saturation vapor pressure over ice to saturation vapor pressure over liquid water (times 100) is represented by the dashed blue line in the center panel.

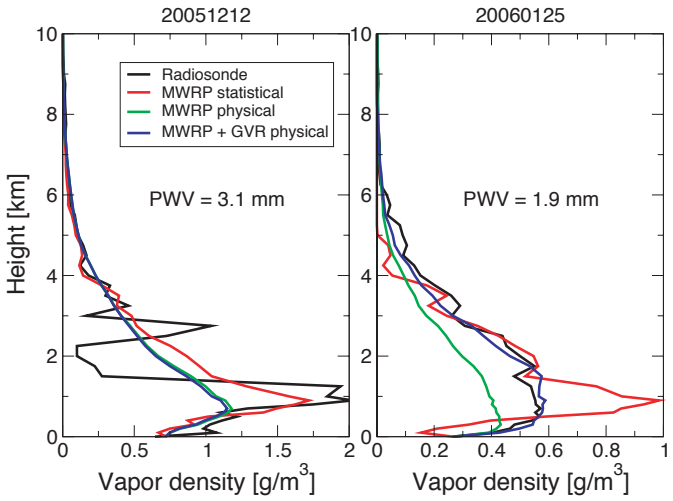

Figure 10. Profiles of water vapor density for 12 December 2005 (left) and 25 January 2006 (right) derived from the MWRP by using a statistical retrieval (red), a physical retrieval (green), with MWRP and GVR combined by using a physical retrieval (blue), and a radiosonde (black).

III. Combined MWRP and 183-GHz Retrievals

Iterative physical retrievals based on the MonoRTM model [13] were developed to derive the water vapor density profiles from K-band measurements of the MWRP and brightness temperatures measured at 183.31 ±1, ±3, ±7, and ±14 GHz with the G-band water vapor radiometer (GVR) [14]. Temperature profiles were derived by using the V-band MWRP channels alone. RMS brightness temperature errors of 2 K were used to account for the observed measured-modeled brightness temperature biases. The results of two cases are presented in Fig. 10. In the first case, 12 December 2005, the additional GVR measurements have no effect. Both physical retrievals produce nearly identical results. The statistical retrieval results may be fortuitous because the brightness temperature biases in Table 1 have not been subtracted here.

In the second case, 25 January 2006, incorporating the GVR measurements into the retrieval clearly improves the result. The reason for the difference in performance between the two cases is that in the first case, the precipitable water vapor (PWV) was more than 3 mm, whereas in the second case, the PWV was less than 2 mm. Above 2 mm PWV, the 183±1 GHz channel begins to saturate and contributes little to the profile retrieval.

IV. Conclusion

Statistical retrievals of temperature and water vapor density profiles have been developed for zenith-only and for multi-angle brightness temperature measurements in the 22- to 30-GHz and 50- to 60-GHz ranges. These have been applied to microwave radiometer measurements from Barrow, Alaska, for 2004-2006. Biases in the measured-modeled brightness temperatures at 51.25, 52.28, and 53.85 GHz, which may be due to spectroscopic issues with the oxygen absorption model, produce biases in both zenith-only and multi-angle temperature retrievals, as predicted by the contribution functions. A small (much less than 0.5°) tilt in the radiometer can significantly bias the brightness temperatures at low elevation angles, but averaging the brightness temperatures from symmetric angles on opposite sides of the zenith alleviates the problem.

For horizontally homogenous, clear sky conditions such that measurements at all angles represent equivalent conditions, the multi-angle retrievals offer better performance in the lowest 1-2 km, though at the cost of increased complexity. Using additional angles may further improve performance.

Utilizing the GVR measurements at 183.31±1, ±3, ±7, and ±14 GHz in addition to the five K-band channels of the MWRP can significantly improve the water vapor density profile retrievals for very low PWV conditions such that the ±1 and ±3 GHz channels retain sensitivity.

References

[1] J. C. Liljegren, "Evaluation of a new multi-frequency microwave radiometer for measuring the vertical distribution of temperature, water vapor, and cloud liquid water," Report ANL/DIS-05-04, Argonne National Laboratory, Argonne, IL, 2002.

[2] J. C. Liljegren, "Automatic self-calibration of ARM microwave radiometers," in *Microwave Radiometry and Remote Sensing of the Earth's Surface and Atmosphere*, P. Pampaloni, S. Paloscia, Eds., Zeist, The Netherlands: VSP Press, 2000, pp. 433-443.

[3] B. L. Gary, "Passive microwave temperature profiler," Report JPL-D-5484, Jet Propulsion Laboratory, California Institute of Technology, Pasadena, CA, 1988.

[4] E. R. Westwater, Y. Han, and F. Solheim, "Resolution and accuracy of a multi-frequency scanning radiometer for temperature profiling," in *Microwave Radiometry and Remote Sensing of the Earth's Surface and*

Atmosphere, P. Pampaloni, S. Paloscia, Eds., Zeist, The Netherlands: VSP Press, 2000, pp. 129-135.

[5] J. A. Schroeder and E. R. Westwater, "Users guide to WPL microwave radiative transfer software," Report ERL-WPL-213, NOAA Environmental Research Laboratory, Boulder, CO, 1991.

[6] P. Rosenkranz, "Water vapor continuum absorption: A comparison of measurements and models," *Radio Sci.*, vol. 33, pp. 919-928, 1998.

[7] P. Rosenkranz, private communication, August 2003.

[8] R. R. Gamache, and J. Fischer, "Half-widths of $H_2{}^{16}O$, $H_2{}^{18}O$, $H_2{}^{17}O$, $HD^{16}O$, and $D_2{}^{16}O$: I. Comparison between isotopomers." *J. Quant. Spectrosc. Radiat. Transfer*, vol. 78, pp. 289-304, 2003.

[9] J. C. Liljegren, S.-A. Boukabara, K. Cady-Pereira, and S. A. Clough, "The effect of the half-width of the 22-GHz water vapor line on retrievals of temperature and water vapor profiles with a 12-channel microwave radiometer," *IEEE Trans. Geosci. and Remote Sens.*, vol. 43, pp. 1102-1108, 2005.

[10] E. J. Mlawer, S. A. Clough, and D. C. Tobin, "The MT_CKD water vapor continuum: A revised perspective including collision induced effects," presented at the *Atmospheric Science from Space Using Fourier Transform Spectrometry (ASSFTS) Workshop*, Bad Wildbad (Black Forest), Germany, 8-10 October 2003.

[11] C. D. Rodgers, *Inverse Methods for Atmospheric Sounding*, Singapore: University Scientific, 2000.

[12] M. P. Cadeddu, K. Kady-Pereira, S. A. Clough, and J. C. Liljegren, "Improving the modeling of oxygen-band absorption: A model-measurement comparison," *Preprints of the 9th Specialists Meeting on Microwave Radiometry and Remote Sensing Applications*, San Juan, Puerto Rico, 28 February-3 March 2006.

[13] S. A. Boukabara, S. A. Clough, and R. N. Hoffman, "MonoRTM: A monochromatic radiative transfer model for microwave and laser calculations," *22nd Annual Review of Atmospheric Transmission Models*, MA, 1999.

[14] M. P. Cadeddu, J. C. Liljegren, and A. Pazmany, "Measurements and retrievals from a new 183-GHz water vapor radiometer in the Arctic," *Preprints of the 9th Specialists Meeting on Microwave Radiometry and Remote Sensing Applications*, San Juan, Puerto Rico, 28 February-3 March, 2006.